

Vacancy-formation energies at the (111) surface and in bulk Al, Cu, Ag, and Rh

H.M. Polatoglou

Physics Department, Aristotle University of Thessaloniki, GR-54006, Greece

M. Methfessel* and M. Scheffler

Fritz-Haber-Institut der Max-Planck-Gesellschaft, Faradayweg 4-6, D-1000 Berlin 33, Germany

(Received 1 February 1993)

The vacancies at the Al, Cu, Ag, and Rh (111) surface are investigated using total-energy and charge-density calculations. For comparison, results of the bulk vacancies are presented as well. In both cases the $(\sqrt{3} \times \sqrt{3})R30^\circ$ surface unit cell is used. The calculations apply density-functional theory together with the local-density approximation and the *ab initio* full-potential linear-muffin-tin-orbital method. The results compare well with known experimental data. In addition, the results are discussed in terms of a tight-binding model in the second moment approximation. It is found that among those metals which are studied here, Al has exceptionally small values for the vacancy-formation energies in the bulk and at the surface. This is related to the formation of a sp^2 bonding component in the Al bonds on the (111) surface for the case of a periodic vacancy structure with a $(\sqrt{3} \times \sqrt{3})R30^\circ$ surface unit cell.

I. INTRODUCTION

The adsorption of alkali-metal atoms on metallic surfaces is interesting, partly because of its strong adsorption-induced electric fields, which imply a technological importance for efficient electrodes (low work function) and for heterogeneous catalysis. Furthermore, alkali metals are prototype systems to study the basic mechanisms of chemisorption¹⁻⁴ because of their simple electronic structure. Until recently, it was generally assumed that alkali-metal adatoms on a close-packed metal surface will occupy a high-coordination site on an otherwise almost perfect substrate. This view has been recently challenged by experimental and theoretical results. More specifically, it was found that for Na adsorbed on the Al(111) surface the configuration with the lowest energy is that of Na replacing an Al surface atom.⁵⁻⁷ The same was shown to hold for K.^{7,8} This process can be thought to occur in the following sequence: (1) formation of a surface Frenkel pair (i.e., a surface vacancy and a substrate adatom), (2) diffusion of the adatom to a kink site at the surface, and (3) adsorption of the Na atom in the vacancy. The sum of the energies of the first two processes gives the formation energy of a surface vacancy, E_f^{vac} .⁷ The surface vacancy-formation energy is endothermic (i.e., $E_f^{\text{vac}} > 0$), while the third step is an exothermic reaction (i.e., $E_3 < 0$). The condition for the realization of the substitutional adsorption is that $\Delta E = E_3 - E_{\text{ad}}^{\text{normal}}$ is negative and lower than $-E_f^{\text{vac}}$. Here with $E_{\text{ad}}^{\text{normal}}$ we denote the energy gained by the adsorption of a Na atom at the perfect surface. From the above, we see that the energy to form surface vacancies is crucial for this process to occur or not.

The substitutional adsorption of Na or K on Al(111) is observed for the $(\sqrt{3} \times \sqrt{3})R30^\circ$ surface unit cell.^{5,8} This

unit cell contains one alkali metal and two Al surface atoms. The surface layer can be thought of as a two-dimensional array of vacancies with a $(\sqrt{3} \times \sqrt{3})R30^\circ$ surface unit cell occupied by Na or K atoms. Theoretical investigations have shown that the main reason for this substitutional adsorption is the unusually low energy required to create surface vacancies with the $(\sqrt{3} \times \sqrt{3})R30^\circ$ structure on Al(111).⁷ With the aim to find other systems which show similar behavior we study the energy needed to create this particular surface-vacancy structure at the (111) surface of different metals, and try to understand if and how this energy relates to the properties of the material. Such a goal can be accomplished by *ab initio* total-energy calculations based on the local-density approximation (LDA).⁹⁻¹¹ As is well known, such techniques give reliable results for the ground-state geometry of a wide variety of systems, including surfaces (see, for example, Refs. 12-15).

We choose the fcc metals Al, Cu, Ag, and Rh and consider the (111) surface, because there already exist results for the alkali-metal adsorption as well as for the vacancy structure on Al(111).^{5,7} Besides Al(111) we study transition metals from the same row of the Periodic Table with filled and partially filled *d* bands (Rh and Ag), and noble metals from different rows (Cu and Ag). In Sec. II we present the theory and the details of the calculations, and in Sec. III the results and the discussion. Section IV is devoted to conclusions.

II. THEORY AND METHOD

In our surface calculations the surface is modeled by a periodically repeated slab.^{14,15} The electronic states and the total energy are calculated using the density-functional theory in the local-density approximation (DFT-LDA),⁹⁻¹¹ where the resulting Kohn-Sham equa-

tion is solved using the full-potential linear-muffin-tin-orbital (FP-LMTO) method.^{16,17} No relativistic corrections were included. The details of how the FP-LMTO method can be used to perform surface calculations are described in Ref. 14.

The lattice constants, obtained from bulk calculations with 499 \mathbf{k} points in the irreducible part of the Brillouin zone, are 7.48, 6.71, 7.74, and 7.19 bohr for Al, Cu, Ag, and Rh, respectively. Later on, in Sec. III, it will be necessary to know the cohesive energy relative to the non-spin-polarized atom (E'_{coh}). The calculated values for the fcc structure are 4.09, 4.47, 3.37, and 7.99 eV/atom for Al, Cu, Ag, and Rh, respectively.

The surface calculations are performed using a slab consisting of seven (111) layers separated by vacuum equivalent to five such layers. The surface unit cell is that of a $(\sqrt{3} \times \sqrt{3})R30^\circ$ structure. We use a truncated-bulk geometry with the above-noted lattice constants. Therefore, surface relaxations are neglected. We expect that they may change our results by ≤ 0.1 eV. An evenly distributed set of \mathbf{k} points is used with seven \mathbf{k} points in the irreducible part of the surface Brillouin zone. For a better numerical stability, each sampled energy is broadened with a Gaussian having $\sigma = 0.3$ eV. For the surface vacancy we remove one surface atom per surface unit cell. The nearest vacancy distance is the distance of the third-nearest neighbors in the bulk metal. The total number of atoms contained in the supercell is 21 and 19 for the perfect slab and for the vacancy system, respectively.

In the present study we want to calculate both the surface and the bulk vacancy applying essentially the same numerical approximations, as, for example, \mathbf{k} summations, energy broadening, and basis functions. As a consequence the energy differences between results for the surface and the bulk vacancies should be particularly accurate. Therefore, the bulk-vacancy calculations are performed for a $(\sqrt{3} \times \sqrt{3})R30^\circ$ vacancy arrangement at the central layer of the slab.

Ab initio calculations provide results which can be related to several physical properties, but they also give results which can be used to test and to determine the parameters of simple empirical models. Such models

can describe the physics of complicated systems in a more economical and intuitive way, albeit with less accuracy and sometimes even with unreliable results. One of the many models, which have been used to describe the metallic bonding, is the tight-binding model in the second moment approximation.^{18,19} In this model the correct total energy of the interacting many-atom system is approximated by the energy per atom as a function of its local coordination number C ,

$$E(C) = E_0 - A\sqrt{C} + BC \quad . \quad (1)$$

Besides a constant, there is an attractive term, which goes as the square root of C and a (typically weak) repulsive term proportional to C . In principle, the coefficients A and B depend, for example, on the interatomic distances, number of electrons, and the local symmetry. Equation (1) is also the essential ingredient of many simplified theories such as the effective-medium theory and the embedded-atom method.¹⁹ The quality of Eq. (1) has been recently studied by performing calculations for several real and hypothetical arrangements of metal atoms, with the same interatomic distance. The coefficients A , B , and E_0 have been determined from least-squares fits of the *ab initio* total energies.^{15,19} It was shown that the surface energies for (111), (100), and (110) surfaces for all 4d elements are more or less well predicted by this model.¹⁵ From these results one may expect that the formation energies of bulk and surface vacancies are also described by the model. We will see that this is not always true.

III. RESULTS AND DISCUSSION

A. Surface properties

For the perfect surface and a 1×1 unit cell, the surface energy is given by the relation, $E_{\text{slab}} = 2E_{\text{surf}} + mE_{\text{bulk}}$. Here, E_{slab} is the total energy of the slab per unit cell, E_{bulk} is the energy per atom in an infinite crystal, E_{surf} is the surface energy, and m is the number of atoms in the slab unit cell. The work function is the minimum en-

TABLE I. Surface energy (σ) and work function (Φ) for the fcc(111) surface.

		Al	Cu	Ag	Rh
σ (J/m ²)	Present work	0.83	1.94	1.21	2.54
	LMTO-ASA calculation ^a	1.27	1.96	1.12	2.78
	Experimental results ^b	1.17	2.02	1.54	
	Experimental results ^c	1.16	1.83	1.25	2.70
Φ (eV)	Present work	4.17	5.10	4.67	5.44
	LMTO-ASA calculation ^a	4.54	5.30	5.91	5.01
	Experimental results ^c	4.24	4.94	4.98	4.74
	Experimental results ^{d,e}	4.30 ^d	4.9 ^e		

^aReference 20.

^bReference 21.

^cReference 22.

^dReference 23.

^eReference 24.

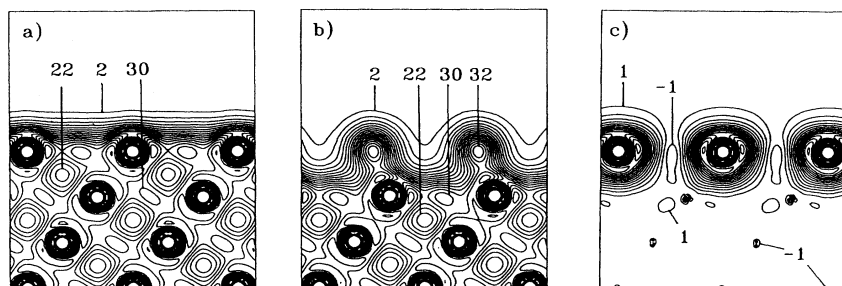


FIG. 1. Valence-electron charge density of Al (a) for a perfect surface, (b) a surface with vacancies, and (c) their difference. The vacancies have the $(\sqrt{3} \times \sqrt{3})R30^\circ$ structure. The plane of the contour plots is normal to the surface and parallel to the $[1\bar{2}1]$ axis. Units are in 10^{-3} bohr $^{-3}$.

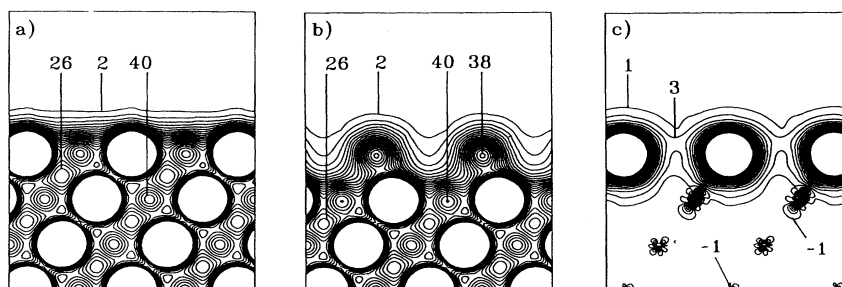


FIG. 2. Same as Fig. 1 but for Cu.

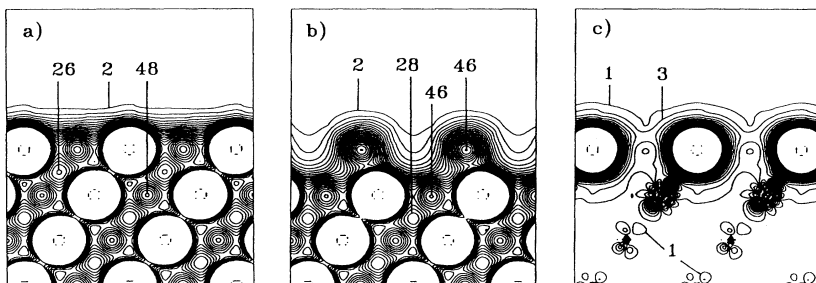


FIG. 3. Same as Fig. 1 but for Rh.

TABLE II. Vacancy-formation energies at the (111) surface (E_f^{vac}) and in the bulk ($E_f^{\text{vac}-b}$). A $(\sqrt{3} \times \sqrt{3})R30^\circ$ structure of vacancies is used. The calculation of Ref. 25 deals with a 27-atom bulk unit cell, and the experimental results refer to the limit of an isolated vacancy.

		Al	Cu	Ag	Rh
E_f^{vac} (eV)	Present results	0.36	0.92	0.67	1.32
	Pseudopotential calculation ^a	0.49			
$E_f^{\text{vac}-b}$ (eV)	Present results	0.57	1.29	1.06	2.26
	Experimental results ^b	0.65	1.04	0.93	1.71
	Experimental results ^c	0.66	1.28	1.11	
	Pseudopotential calculation ^d	0.56			

^aReference 7.

^bReference 22.

^cReference 26.

^dReference 25.

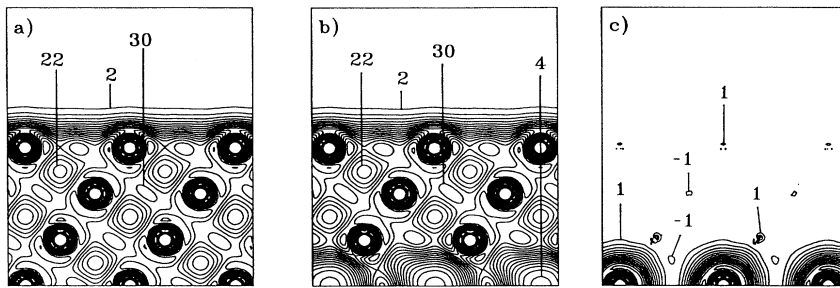


FIG. 4. Valence-electron charge density of Al (a) for a perfect slab, (b) a slab with vacancies in the central layer, and (c) their difference. The vacancies have the $(\sqrt{3} \times \sqrt{3})R30^\circ$ structure. The plane of the contour plots is normal to the surface and parallel to the $[1\bar{2}1]$ axis. Units are in 10^{-3} bohr $^{-3}$.

ergy to remove one electron from the slab. It is obtained by the difference of the potential in the vacuum and the Fermi energy. In Table I we present the calculated properties, results of other calculations and experimental data. The most recent complete theoretical calculations have been performed using the FP-LMTO (Ref. 14) and the Green-function LMTO method in the atomic-sphere approximation (ASA).²⁰ We do not present values from the former because they are identical with the present results. It is to be noted that the experimental data for the (111) surface energy are not known, and that these data in Table I refer to some (unclear) average of several low index planes of the crystal surfaces or to liquid metals. Therefore the experimental data for the surface energy should have, in general, higher values than the calculated ones. The comparison shows that the agreement between the different theoretical results and the experimental data is good.

B. Surface-vacancy calculation

In view of recent theoretical and experimental findings about the alkali-metal adsorption on Al(111) we studied a $(\sqrt{3} \times \sqrt{3})R30^\circ$ structure of surface vacancies. As mentioned before, this structure was found to actuate the adsorption and island formation of Na and K on Al(111).⁷ In the following we will analyze the properties of this vacancy structure for Al, Cu, Ag, and Rh. The distance between nearest vacancies equals the distance between an atom and its third-nearest neighbors in the bulk. Because screening in metals is very effective one may expect that the different vacancies are coupled only weakly. In Figs. 1, 2, and 3 we show the calculated charge density of

the perfect surface, the surface with vacancies and their difference for Al, Cu, and Rh. We observe that indeed the charge-density perturbation induced by the surface vacancies is rather localized reaching only slightly farther than the nearest-neighbor atoms. The charge density in the core region is high because we use the true wave function, i.e., no pseudopotential approach as in Ref. 7. As a consequence, the perturbation of the charge density close to the nuclei is only a tiny fraction of the unperturbed density, although it looks quite sizable. Furthermore, it can be seen that the strength of the perturbation increases in the sequence Al, Cu, and Rh.

The calculated values for the surface-vacancy-formation energies are given in Table II along with the result for Al, obtained using the *ab initio* pseudopotential method and the same vacancy structure.⁷ The agreement between the present FP-LMTO calculation and the previous pseudopotential calculation is satisfactory.

C. Bulk-vacancy calculation

We use the same supercell as in Sec. IIB, but now we remove one atom per $(\sqrt{3} \times \sqrt{3})R30^\circ$ unit cell from the central layer of the slab. In Figs. 4–6 we show the charge density of the perfect slab, the slab with the vacancies, and the difference between the two for Al, Cu, and Rh. Similar as for the surface vacancies, the perturbation in the charge density is very localized. In Table II we include the values for the bulk-vacancy-formation energy ($E_f^{\text{vac}-b}$) along with known experimental data. Also we include the previous theoretical result for Al obtained by the pseudopotential method.²⁵ The agreement with experimental results is quite good and in some cases excellent. Furthermore, the agreement between the previous

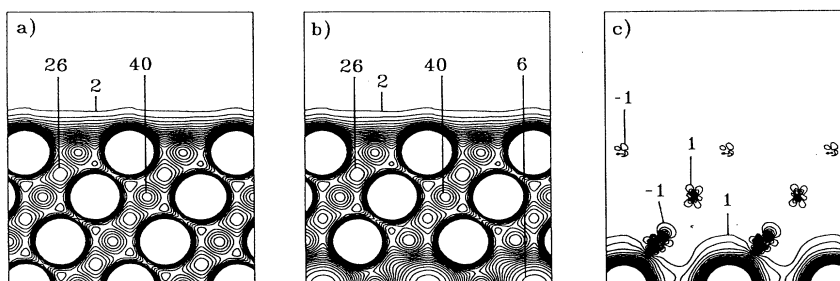


FIG. 5. Same as Fig. 4 but for Cu.

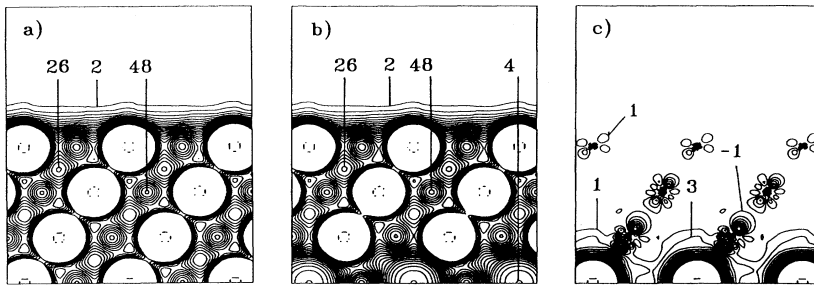


FIG. 6. Same as Fig. 4 but for Rh.

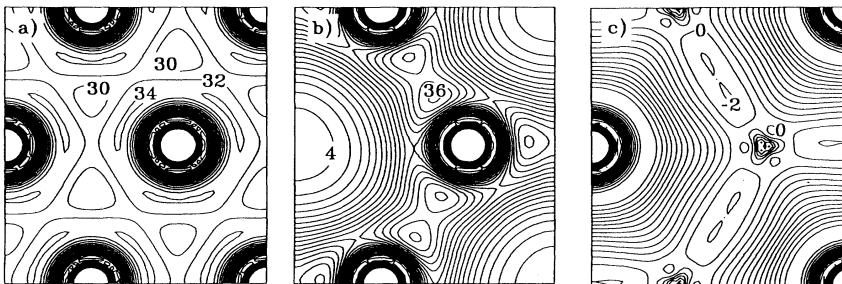
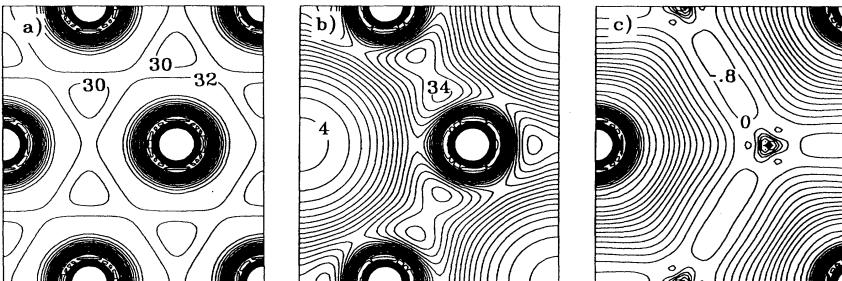
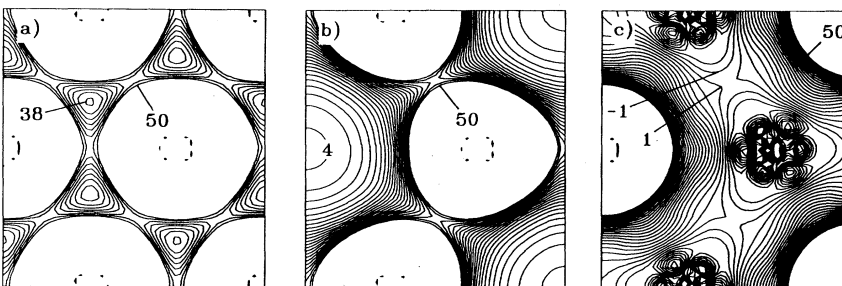
FIG. 7. Valence-electron charge density of Al (a) for a perfect surface, (b) a surface with vacancies, and (c) their difference. The vacancies have the $(\sqrt{3} \times \sqrt{3})R30^\circ$ structure. The plane of the contour plots is the surface atomic plane, i.e., a [111] plane. Units are in $10^{-3} \text{ bohr}^{-3}$.FIG. 8. Valence-electron charge density of Al (a) for a perfect slab, (b) a slab with a vacancy in the central layer, and (c) their difference. The vacancies have the $(\sqrt{3} \times \sqrt{3})R30^\circ$ structure. The plane of the contour plots is the central atomic plane, i.e., a [111] plane. Units are in $10^{-3} \text{ bohr}^{-3}$.

FIG. 9. Same as Fig. 7 but for Rh.

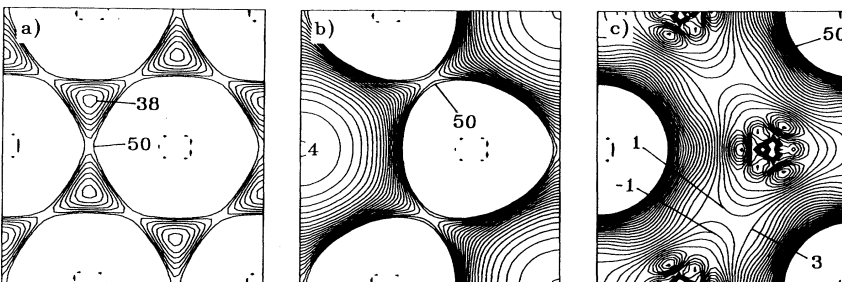


FIG. 10. Same as Fig. 8 but for Rh.

TABLE III. Surface energies (σ) and formation energies for a $(\sqrt{3} \times \sqrt{3})R30^\circ$ arrangement of bulk vacancies $E_f^{\text{vac}-b}$ and of surface vacancies E_f^{vac} . The *ab initio* results are from the present calculation and the simple model ones are obtained using Eq. (1) and the parameters given in Eq. (2).

		Al	Cu	Ag	Rh
σ (J/m ²)	<i>ab initio</i>	0.83	1.94	1.21	2.54
	Simple model	0.90	1.19	0.65	1.94
$E_f^{\text{vac}-b}$ (eV)	<i>ab initio</i>	0.57	1.29	1.06	2.26
	Simple model	1.37	1.50	1.13	2.61
E_f^{vac} (eV)	<i>ab initio</i>	0.36	0.92	0.67	1.32
	Simple model	0.88	0.97	0.73	1.75

pseudopotential calculation and the present FP-LMTO calculation is very good.

D. Discussion

It is always desirable to find a simple way to account for the energies and the trends in the results of a full-scale microscopic, quantum-mechanical calculation. The aim of the present section is to compare results of the simple bond-strength–coordination-number model [see Eq. (1)] to the full *ab initio* calculations. The parameters of the tight-binding model are determined as follows:

$$\begin{aligned}
 E_0 &= 0, \\
 E(12) &= -E'_{\text{coh}}, \\
 B &= 0.03E'_{\text{coh}},
 \end{aligned} \tag{2}$$

where, as mentioned before, E'_{coh} is the calculated cohesive energy relative to the non-spin-polarized atom. The constant E_0 is set to zero because it does not play any role, as we are only interested in energy differences. This choice of parameters has been previously used for the surface energy of the $4d$ transition metals,¹⁵ where it was shown to give similar results for the surface energies as the full *ab initio* calculations.

In Table III we present results for the surface energy, bulk, and surface-vacancy-formation energies. Comparison of the simple model with the full-scale calculations shows that there is a fair agreement for the surface energies, but particularly large discrepancies occur for E_f^{vac} of Rh and Ag, and even larger for the E_f^{vac} and $E_f^{\text{vac}-b}$ of Al. This means that for those cases where the deviations are large there are effects, like charge redistribution, which cannot be accounted for by the simple model.

In Fig. 7 the charge density of Al along the surface atomic plane is depicted for the cases of the perfect surface, the surface with vacancies, and the difference of the two. It can be seen that the vacancies induce an accumulation of charge in the nearest-neighbor bonds. The corresponding results for the bulk vacancy are shown in Fig. 8. For this case the qualitative electron charge-

density change is similar, but quantitatively the accumulation is less pronounced. It is interesting to note that the $(\sqrt{3} \times \sqrt{3})R30^\circ$ vacancy structure implies a graphitic structure of the remaining atoms in the layer. In fact, the above results can be thought of as the realization of an sp^2 type of bonding which is favored by the considered geometry. Obviously, the comparison with graphite has some limitations, because here we consider only a single layer of “graphitic aluminum” on (or in) an otherwise fcc Al crystal.

It is interesting to see whether similar effects occur for metals whose bonding is partly due to d electrons. In particular, we study the case of Rh. The results are given in Figs. 9 and 10. It can be noticed that due to the vacancies a small amount of charge flows away from the Rh bonds. Compared to Al the effect is in the opposite direction and much smaller in view of the large difference in the number of valence electrons. Therefore, the exceptional behavior of Al can be ascribed to the geometry of the atoms at the $(\sqrt{3} \times \sqrt{3})R30^\circ$ surface in the presence of vacancies and to the sp bonding character of Al. Aluminum is typically called a “jelliumlike” system. However, the results show that it is very close to a covalent one. If it is placed in a different local environment, clearly localized, directional bonds are formed. Of course, this is known about molecules as well as about III-V semiconductors. For the pure aluminum system the strength of the effect is somehow surprising.

IV. CONCLUSIONS

The vacancies in the bulk and at the (111) surface of Al, Cu, Ag, and Rh have been studied, using a repeated slab with the $(\sqrt{3} \times \sqrt{3})R30^\circ$ surface unit cell. The bulk-vacancy-formation energies are in good agreement with known experimental data. Comparison of the estimates of a simple tight-binding second moment model shows large deviations for the bulk-vacancy-formation energy of Al and for the surface-vacancy-formation energy of all the studied metals. The largest deviation is for the case of Al. It is found that the geometry of the $(\sqrt{3} \times \sqrt{3})R30^\circ$ surface unit cell and the occupied s and p bonding orbitals make it possible for the in-plane Al bonds to acquire an sp^2 bonding component. The other metals do not show such an effect. However, the present results seem to indicate that for the considered structure there exists appreciable interaction between the surface vacancies. It seems that silver is a good choice for studying in detail such an interaction.

ACKNOWLEDGMENTS

One of the authors (H.M.P.) would like to thank the Fritz-Haber-Institut for supporting his visit there, during which parts of this work have been performed, and to acknowledge partial support by the EEC Science Program No. SC1-CT91-0703 (TSTS).

- *Permanent address: Institut für Halbleiterphysik, Frankfurt an der Oder, Germany.
- ¹J.B. Taylor and I. Langmuir, *Phys. Rev.* **44**, 423 (1933).
- ²R.W. Gurney, *Phys. Rev.* **47**, 479 (1935).
- ³N.D. Lang and A.R. Williams, *Phys. Rev. B* **18**, 616 (1978).
- ⁴*Physics and Chemistry of Alkali Metal Adsorption*, edited by H.P. Bonzel, A.M. Bradshaw, and G. Ertl (Elsevier, Amsterdam, 1989).
- ⁵A. Schmalz, S. Aminpirooz, L. Becker, J. Haase, J. Neugebauer, M. Scheffler, D.R. Batchelor, D.L. Adams, and E. Bogh, *Phys. Rev. Lett.* **67**, 2163 (1991).
- ⁶J.N. Andersen, M. Qvarford, R. Nyholm, J.F. van Acker, and E. Lundgren, *Phys. Rev. Lett.* **68**, 94 (1992).
- ⁷J. Neugebauer and M. Scheffler, *Phys. Rev. B* **46**, 16 067 (1992).
- ⁸C. Stampfl, M. Scheffler, H. Over, J. Burchhardt, M. Nielsen, D.L. Adams, and W. Moritz, *Phys. Rev. Lett.* **69**, 1532 (1992).
- ⁹W. Kohn and L.J. Sham, *Phys. Rev.* **140**, A1133 (1965).
- ¹⁰D.M. Ceperley and B.J. Alder, *Phys. Rev. Lett.* **45**, 566 (1980).
- ¹¹J. Perdew and A. Zunger, *Phys. Rev. B* **23**, 5048 (1981).
- ¹²K.M. Ho and K.P. Bohnen, *Phys. Rev. B* **32**, 3446 (1985).
- ¹³D.R. Hamann and P.J. Feibelman, *Phys. Rev. B* **37**, 3847 (1988).
- ¹⁴M. Methfessel, D. Hennig, and M. Scheffler, *Phys. Rev. B* **46**, 4816 (1992).
- ¹⁵M. Methfessel, D. Hennig, and M. Scheffler, *Appl. Phys. A* **55**, 442 (1992).
- ¹⁶M. Methfessel, *Phys. Rev. B* **38**, 1537 (1988).
- ¹⁷M. Methfessel, C.O. Rodriguez, and O.K. Andersen, *Phys. Rev. B* **40**, 2009 (1989).
- ¹⁸V. Heine, in *Solid State Physics*, edited by H. Ehrenreich, F. Seitz, and D. Turnbull (Academic, New York, 1980), Vol. 35, p. 80.
- ¹⁹I.J. Robertson, M.C. Payne, and V. Heine, *Europhys. Lett.* **15**, 301 (1991).
- ²⁰H.L. Skriver and N.M. Rosengaard, *Phys. Rev. B* **46**, 7157 (1992).
- ²¹H. Wawra, *Z. Metallk.* **66**, 395 (1975); **66**, 492 (1975).
- ²²F.R. de Boer, R. Boom, W.C.M. Mattens, A.R. Miedema, and A.K. Niessen, *Cohesion in Metals* (North-Holland, Amsterdam, 1988).
- ²³H.B. Shore and J.H. Rose, *Phys. Rev. Lett.* **66**, 2519 (1991).
- ²⁴N. Fischer, S. Schuppler, R. Fischer, Th. Fauster, and W. Steinmann (unpublished).
- ²⁵M.J. Gillan, *J. Phys. Condens. Matter* **1**, 689 (1989).
- ²⁶H.E. Schaefer, *Phys. Status Solidi A* **102**, 47 (1987).